Supporting Information for: Evolution of the structure of lipid nanoparticles for nucleic acid delivery: From *in situ* studies of formulation to colloidal stability

Jennifer Gilbert,[†,‡] Federica Sebastiani,[†,¶] Marianna Yanez Arteta,[§] Ann Terry,[‖] Anna Fornell,[‖] Najet Mahmoudi,[⊥] and Tommy Nylander[*,†,‡,#,@]

†*Division of Physical Chemistry, Department of Chemistry, Lund University, 221 00 Lund, Sweden.*

‡*NanoLund, Lund University, Professorsgatan 1, 223 63 Lund, Sweden.*

¶*Department of Pharmacy, University of Copenhagen, Universitetsparken 2, 2100 København Ø, Denmark.*

§*Advanced Drug Delivery, Pharmaceutical Sciences, R&D, AstraZeneca, 431 83 Gothenburg, Sweden.*

‖*MAX IV Laboratory, Lund University, Fotongatan 2, 224 84 Lund, Sweden.*

⊥*ISIS Neutron and Muon Source, Harwell Science and Innovation Campus, Didcot OX11 0DE, U.K.*

#*LINXS Institute of Advanced Neutron and X-Ray Science, Lund, Sweden.*

@*School of Chemical Engineering and Translational Nanobioscience Research Center, Sungkyunkwan University, Suwon, Republic of Korea.*

E-mail: tommy.nylander@fkem1.lu.se

Peak fitting for *in situ* and static SAXS measurements of LNPs during mixing and dialysis

The peaks visible in the SAXS data measured during dialysis were fit with the broad_peak model in SasView within a very limited q range, as shown in Fig S1. The fixed parameters were as follows: scale = 1 (fixed), porod_scale = 0 (fixed), lorentz_exp = 2 (fixed). lorentz_scale, lorentz_length, half width half maximum (HWHM) and peak_pos were manually estimated then were fit simultaneously.

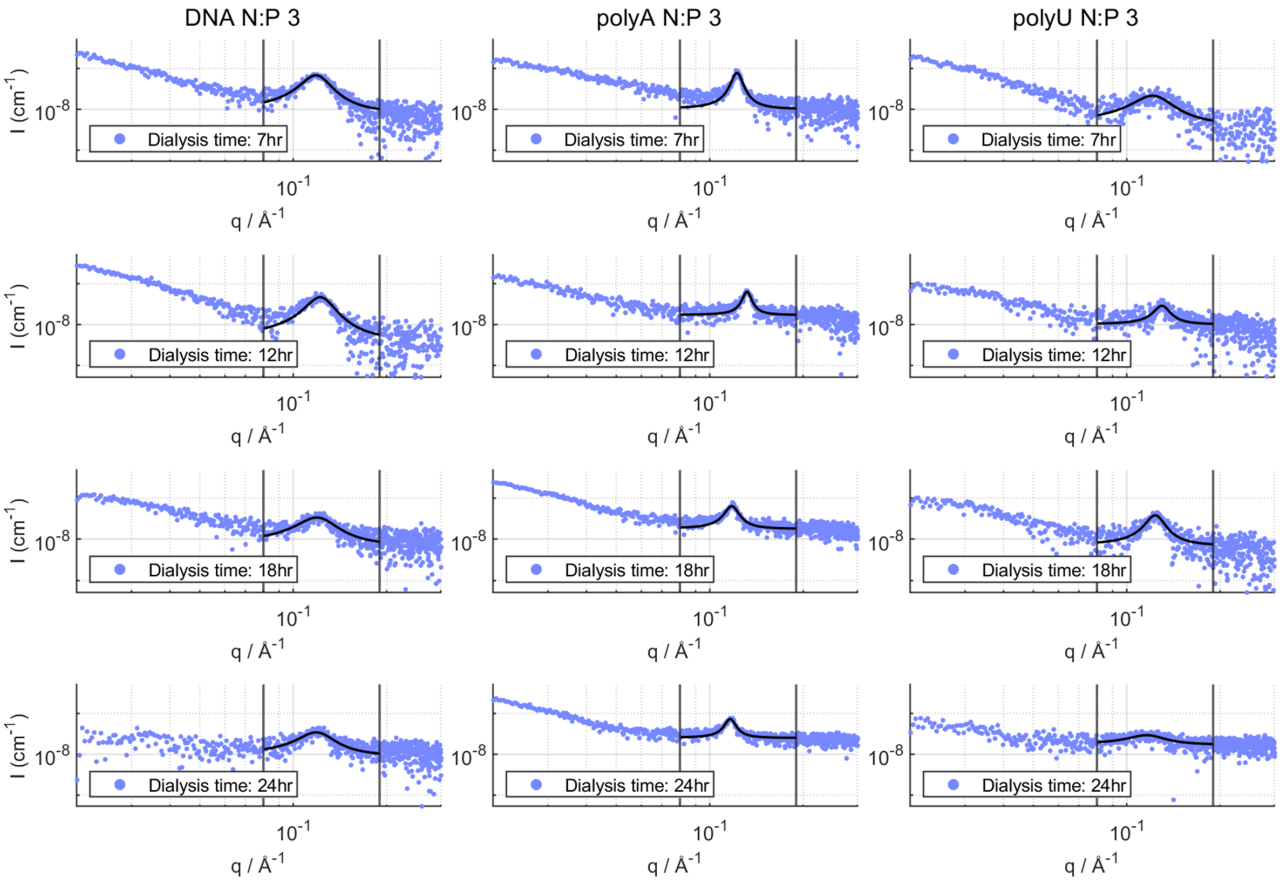

Figure S1: All peaks present in the SAXS data for the LNP formulations during dialysis were fit with a broad peak model in a q range limited to close to the peak position.

Table S1: Fit parameters for DNA N:P 3 LNP SAXS data recorded during dialysis

DNA N:P 3	**Outlet**	**7 hrs**	**12 hrs**	**18 hrs**	**24 hrs**
lorentz_scale$\pm 1\text{x}10^{-10}$	$4.3\text{x}10^{-9}$	$5.99\text{x}10^{-8}$	$4.25\text{x}10^{-8}$	$2.71\text{x}10^{-8}$	$2.53\text{x}10^{-8}$
lorentz_length± 1 /Å	50	74	74	54	58
HWHM± 0.002 /Å^{-1}	0.020	0.014	0.013	0.019	0.017
peak_pos± 0.002 /Å^{-1}	0.109	0.118	0.122	0.119	0.118
d spacing± 1 /Å	58	53	52	53	53

Table S2: Fit parameters for polyA N:P 3 LNP SAXS data recorded during dialysis

polyA N:P 3	**Outlet**	**7 hrs**	**12 hrs**	**18 hrs**	**24 hrs**
lorentz_scale$\pm 1\text{x}10^{-10}$	-	$6.75\text{x}10^{-8}$	$4.64\text{x}10^{-8}$	$4.66\text{x}10^{-8}$	$4.75\text{x}10^{-8}$
lorentz_length± 1 /Å	-	185	209	151	187
HWHM± 0.002 /Å^{-1}	-	0.005	0.005	0.007	0.005
peak_pos± 0.002 /Å^{-1}	-	0.112	0.132	0.118	0.116
d spacing± 1 /Å	-	51	48	54	54

Table S3: Fit parameters for polyU N:P 3 LNP SAXS data recorded during dialysis

polyU N:P 3	**Outlet**	**7 hrs**	**12 hrs**	**18 hrs**	**24 hrs**
lorentz_scale$\pm 1\text{x}10^{-10}$	-	$1.74\text{x}10^{-8}$	$1.86\text{x}10^{-8}$	$3.16\text{x}10^{-8}$	$1.22\text{x}10^{-8}$
lorentz_length± 1 /Å	-	52	116	107	53
HWHM± 0.002 /Å^{-1}	-	0.019	0.009	0.009	0.019
peak_pos± 0.002 /Å^{-1}	-	0.121	0.130	0.123	0.116
d spacing± 1 /Å	-	52	49	51	54

Analysis of cryoTEM images

CryoTEM images were acquired for the following samples to inform the model choice for SANS and provide some initial guesses for the fitting parameters. In addition, fast Fourier transforms (FFT) were performed on the particle core in order to confirm that the peak observed in SAXS and SANS had the same dimensions as the repeat structures observed in the cryoTEM images for some of the samples. The following images show some representative cryoTEM images. Examples of the particles used in the FFTs are included below, with the area of the particle used for the FFT highlighted with a yellow circle and the corresponding FFT with the distance to the spots highlighted with a red arrow.

For the DNA N:P 3 sample, the inner core structure was more visible and spots were observed in the FFTs. Unfortunately for the polyA N:P 3 and polyU N:P 3 samples, the large number of ice crystals limited any in depth analysis of the images, however it was still possible to see something of the structures in the polyU sample and there are spots in FFTs from the polyA samples that agree well with the repeat distance derived from the SAXS data.

DNA N:P 3

For the particles with visible spots in the FFT, the repeat distance was 55±4Å.

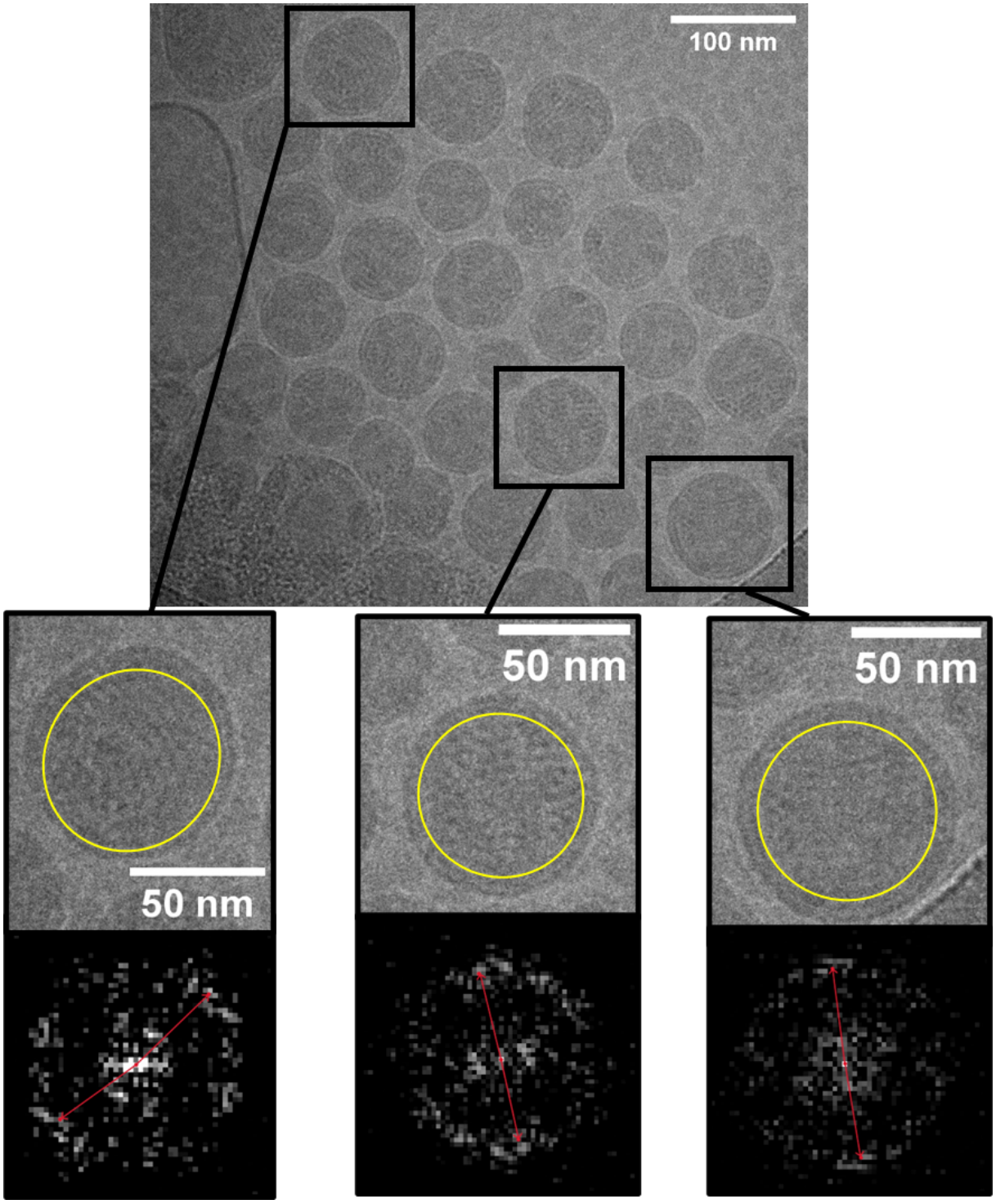

Figure S2: Example cryoTEM images and FFTs for DNA N:P 3.

polyA N:P 3

Although there was a large number of ice crystals, FFTs of the internal structure of the particles produced a repeat distance of 54±4Å, which is in good agreement with the corresponding SAXS data. Although most of the particles in this sample appear as spherical and uniform, there are LNPs highlighted here which appear to have blebs on the surface, similar to those observed in work by Cheng et al.[1]

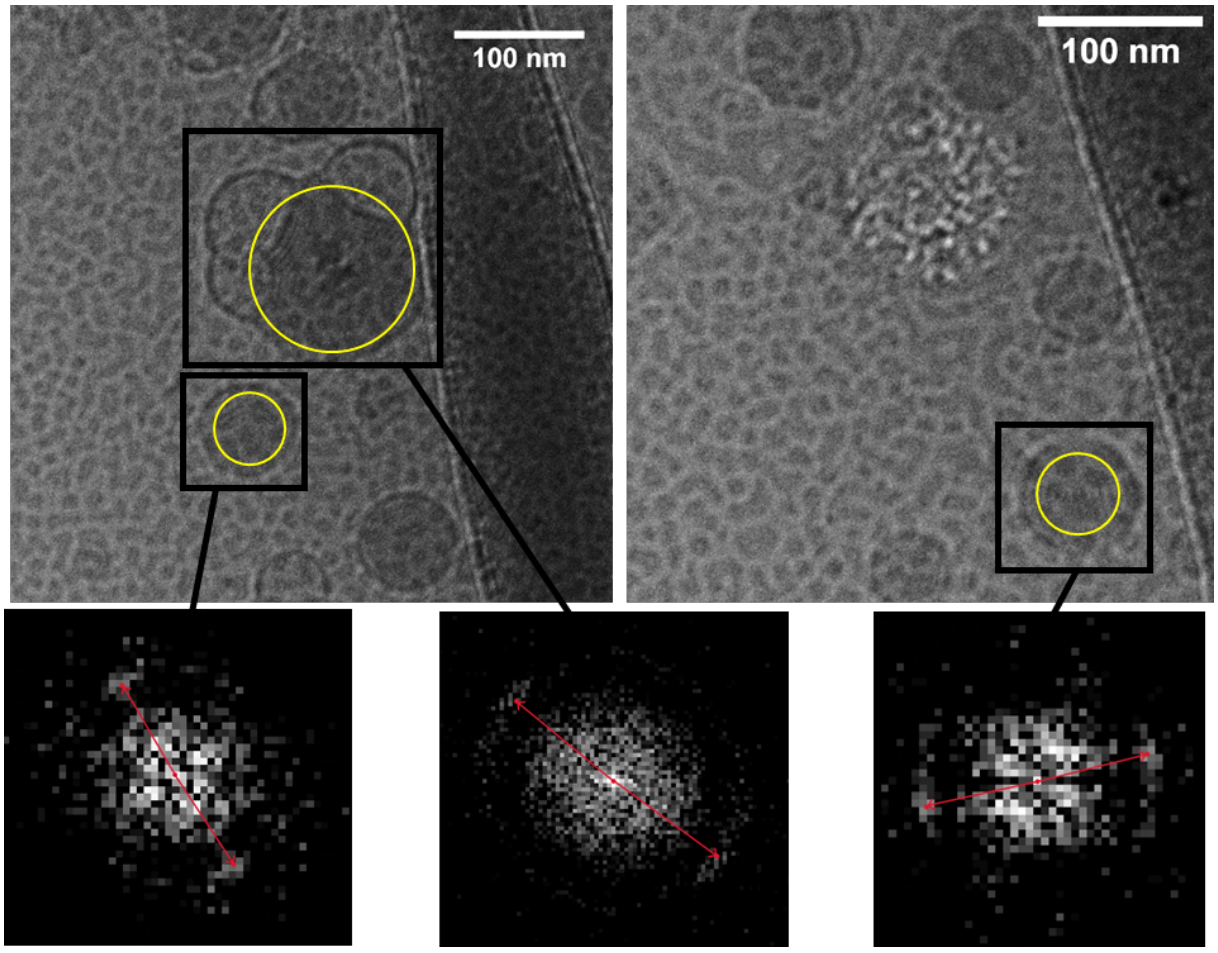

Figure S3: Example cryoTEM images and FFTs for polyA N:P 3.

polyU N:P 3

Although ice quality and ice crystal formation limited the analysis here, it was possible to see a combination of different structures. The uniform spherical structures with a dark interior

appeared similar to the other LNP formulations. However, there were additional oblate structures with a more electron dense shell, which were not observed in any other samples.

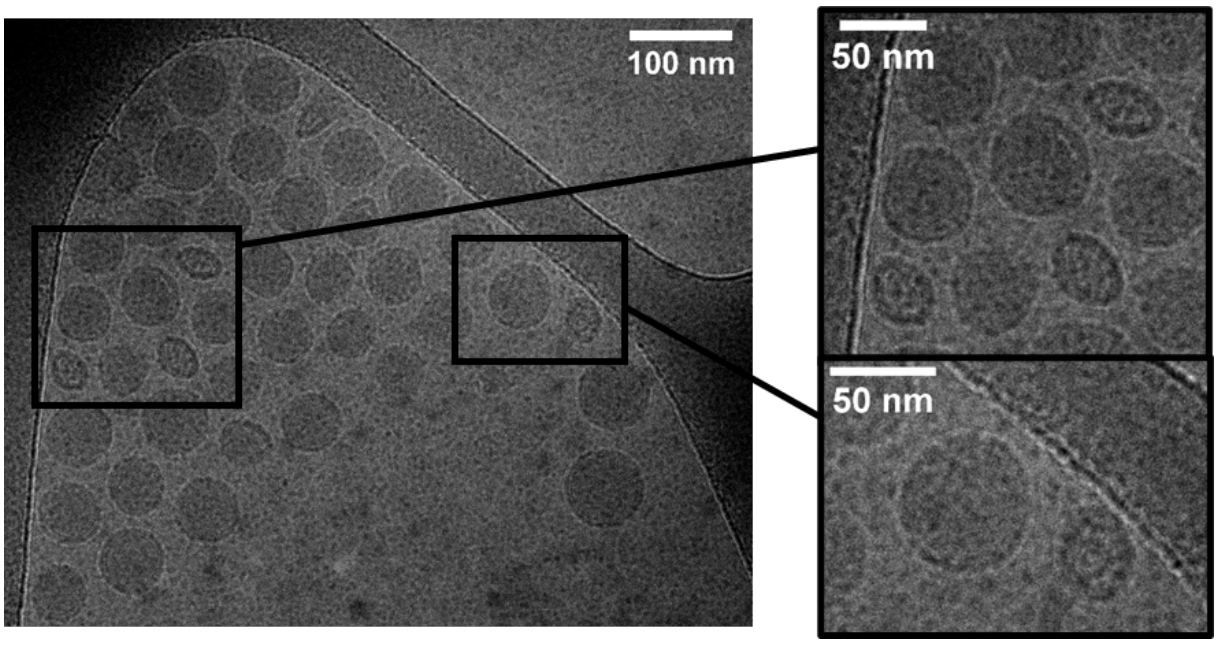

Figure S4: Example cryoTEM images for polyU N:P 3.

SANS Fitting

Calculation of SLD values

All scattering length density values (SLDs) for the water and lipid components were calculated using the NIST Neutron activation and scattering calculator (https://www.ncnr.nist.gov/resources/activation/) using the input values in Table S4.

All SLDs for the nucleic acids were calculated using the STFC ISIS Protein Scattering Length Density Calculator (http://psldc.isis.rl.ac.uk/Psldc/licence.html). For DNA, an equal number of A, G, T and C bases was assumed and the input sequence length taken from the mean of the range provided in the Sigma Aldrich certificate of analysis (708 bp), whereas for polyA and polyU, the input sequence length was 700, approximating the equivalent length. In all cases, the SLD was

calculated assuming 100% H_2O in the solution and 0% deuteration.

Table S4: Calculated SLDs and molecular volumes for LNP components.

Components of LNP	**Input formula**	**Molecular volume /A^3**	**Neutron SLD /10^{-6}Å^{-2}**
H_2O	H2O	30	-0.559
D_2O	D2O	30	6.364
DLin-MC3-DMA (MC3)	C43H79NO2	1290[a]	0.087
hChol	C27H46O[b]	630[c]	0.209
d45Chol (85% D purity)	C27H7.75OD38.25[d]	630[c]	6.536
DSPC	C44H88NO8P[b]	1326[e]	0.202
DMPE(-PEG2000)	C33H66NO8P	1026[f]	0.325
DNA (nt)	-	309	3.175
polyA (nt)	-	314	3.576
polyU (nt)	-	282	3.287

[a]Calculated from the density in Arteta et al.[2]

[b]Molecular formula taken from Avanti Lipids product information.

[c]From Greenwood et al.[3]

[d]d45 cholesterol was kindly synthesised by the National Deuteration Facility (ANSTO, Proposal NDF8442). From the certificate of analysis, the isotopic purity was 85±2%D.

[e]Calculated using the molecular volumes in Armen et al.[4]

[f]Tail volume calculated using the molecular volumes in Armen et al.[4] and head group volume from Wilkinson and Nagle[5].

Model free analysis: Guinier approximation and P(r) inversion

Guinier approximation

Using Guinier's approximation at low q[6], the radius of gyration of a particle, R_g, can be calculated:

$$I(q) \approx I(0) \exp^{\frac{-q^2 R_g^2}{3}} \tag{1}$$

Which can be linearised to:

$$\ln I(q) \approx \frac{-q^2 R_g^2}{3} + \ln I(0) \tag{2}$$

The Guinier approximation is valid only in a limited q range defined by the R_g[6,7]:

(i) The lower limit is given by $q_{min}R_g < 0.65$, which is lower than the lowest q value measured here.

(ii) The upper limit for spherical objects is given by $q_{max}R_g \approx 1.3$, which is indicated in Figure S5 by the black dashed line.

Given the size of the LNPs measured here, the Guinier region in the measured q range was very limited and there were large errors on the lowest data points, therefore the fit was strongly influenced by small deviations of the data from linearity. Although the R_g calculated from the Guinier analysis for the polyA and DNA samples reproduced the expected trend in size observed in DLS, the high error on the fit for DNA and polyA samples and exclusion of the effect of polydispersity limits any in depth interpretation. In the case of the polyU samples, the low q upturn observed due to the aggregation in the sample obscures the Guinier region, therefore it was not possible to fit this data. The solid black line plotted in Figure S5C,D is included only to highlight the low q upturn.

Distance distribution function P(r)

The distance distribution function, P(r), can also be used to characterise the size and shape of a particle[7,8]. The SANS data for the samples were fitted in Sasview in a q range excluding the low q upturn ($q < 0.0035 Å^{-1}$) and the broad peak due to the internal particle structure at $\approx 0.1^{-1}$ and the value of D_{max} was manually optimised (typically 1000 - 1200 Å). For all samples and all solvent contrasts, the P(r) has the bell shape curve typical of a sphere. There is some asymmetry in the curves, which is more visible in the higher $\%D_2O$ contrasts. This could be due to; (i) the core-shell structure of the sphere and/or (ii) the polydispersity of the samples, as this typically results in a tail on the higher r side of the curve and is more

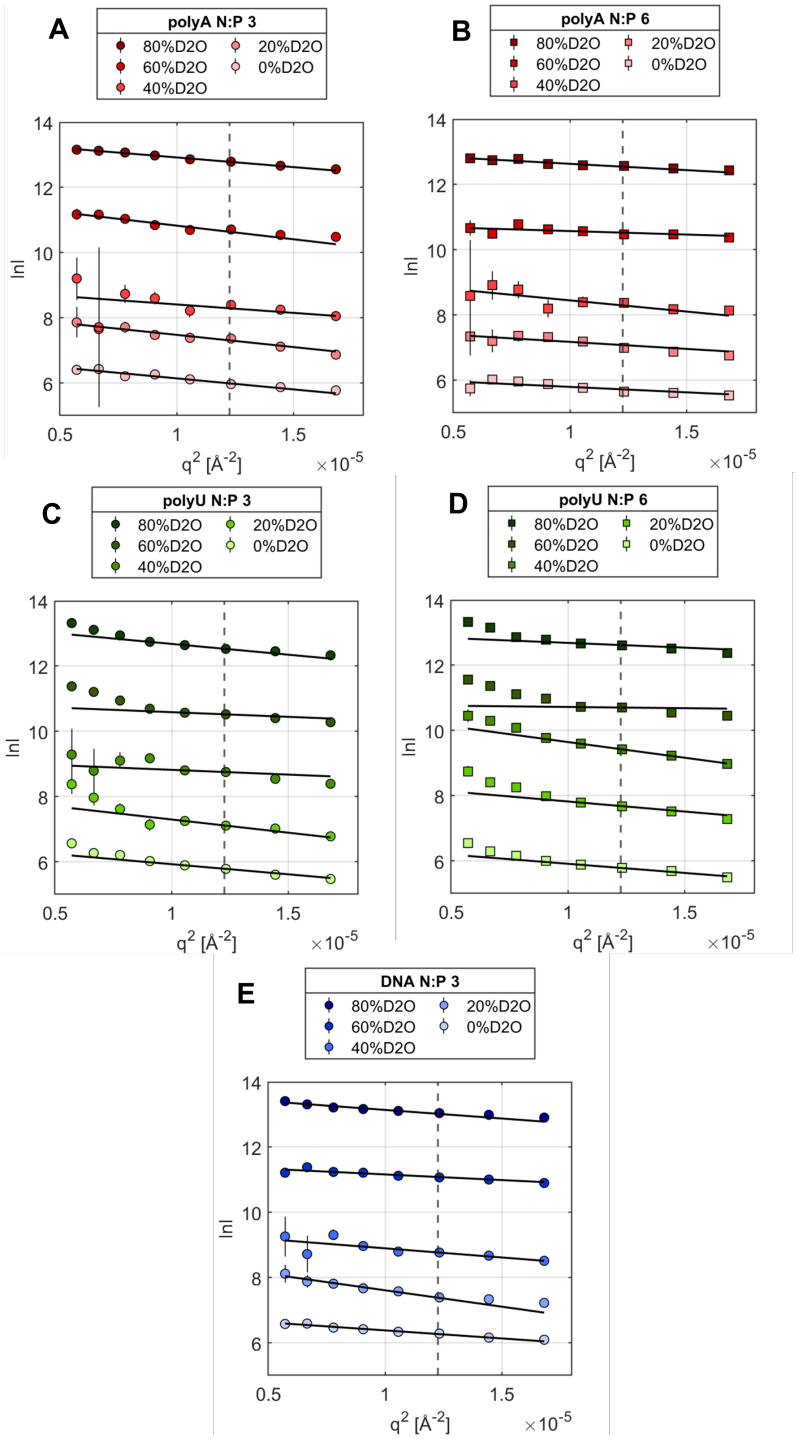

Figure S5: The low q region of the SANS data for the polyA N:P 3 (A) and 6 (B) and the DNA N:P 3 (E) samples were fitted with the linearised equation of Guinier approximation (solid black line). The data for the polyU N:P 3 (C) and 6 (D) samples has a low q upturn due to aggregation which obscures the Guinier region, which is highlighted by the solid black line (please note this is only to guide the eye). The upper limit for the Guinier region is indicated by the black dotted line. All samples were measured in five different solvent contrasts: 0, 20, 40, 60, 80% D_2O (plotted with light to dark colours for increasing D_2O amount). The data are offset for clarity.

prominent in the polyA and polyU samples, which have a higher polydispersity than the DNA sample. The R_g of the particle can also be calculated from the P(r), which changes with contrast following the expected trends from more detailed fitting with a core-shell sphere model described below. The zero average contrast for the lipid composition and cargo used is at ≈35% D_2O and the particle core is matched out at ≈20% D_2O, resulting in low intensity for 20% D_2O and 40% D_2O. The comparison between the R_g calculated from the 0% D_2O data compared to the higher (60, 80%) D_2O contrasts can be attributed to the shell of the core-shell sphere. The contrast between the shell and solvent is low at the higher %D_2O (60, 80%), therefore the shell is not very visible in these solvent contrasts and the calculated R_g is lower. In the 0% D_2O contrast, however, there is good contrast between the shell and solvent, therefore the shell is visible resulting in a higher R_g.

Model description and fitting method

SANS data was fit with a core_shell sphere model plus a broad_peak model (CSS+BP) for all samples, with the initial parameters for the model defined using *a priori* knowledge as much as possible. The data was first fit in a limited range using the core shell sphere (CSS) model only, with an upper q limit of 0.25 $Å^{-1}$. The following parameters were estimated and fixed for each sample:

(i) The scale was estimated based on the calculated LNP concentration (3.9 mg/mL)

(ii) The background was individually estimated for each dataset

(iii) The solvent SLD for each contrast was calculated from the ratio of D_2O/H_2O used to make it (0, 20, 40, 60, 80% D_2O).

(iv) Polydispersity with the Schulz distribution was estimated from the data and fixed at that value for all solvent contrasts.

The following parameters were fitted:

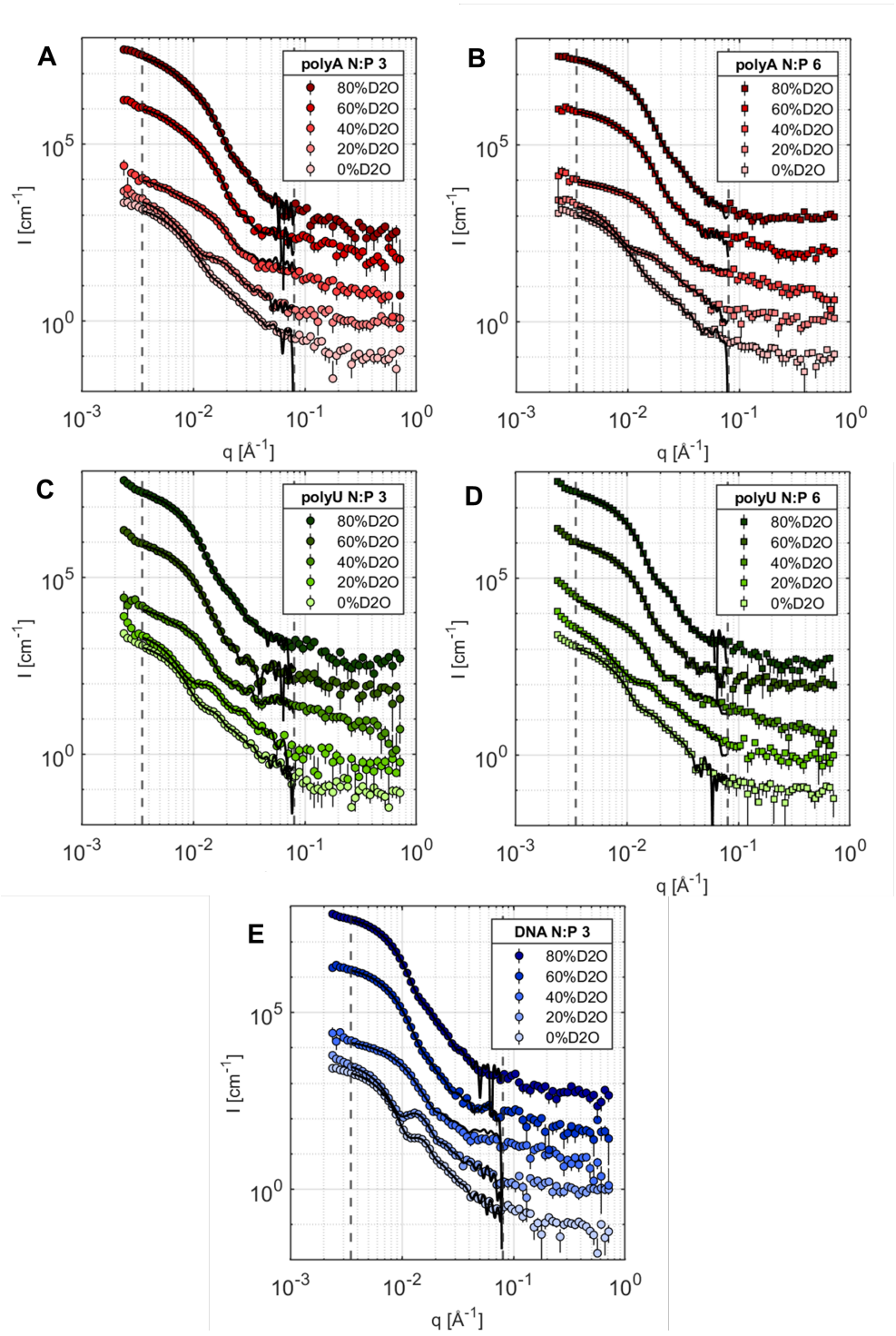

Figure S6: SANS data collected for LNPs containing polyA N:P 3 (A) and 6 (B), polyU N:P 3 (C) and 6 (D) and DNA N:P 3 (E) with the fit corresponding to the P(r) inversion plotted as a solid black line. The fitted q range is indicated by vertical dashed lines and the data are offset for clarity.

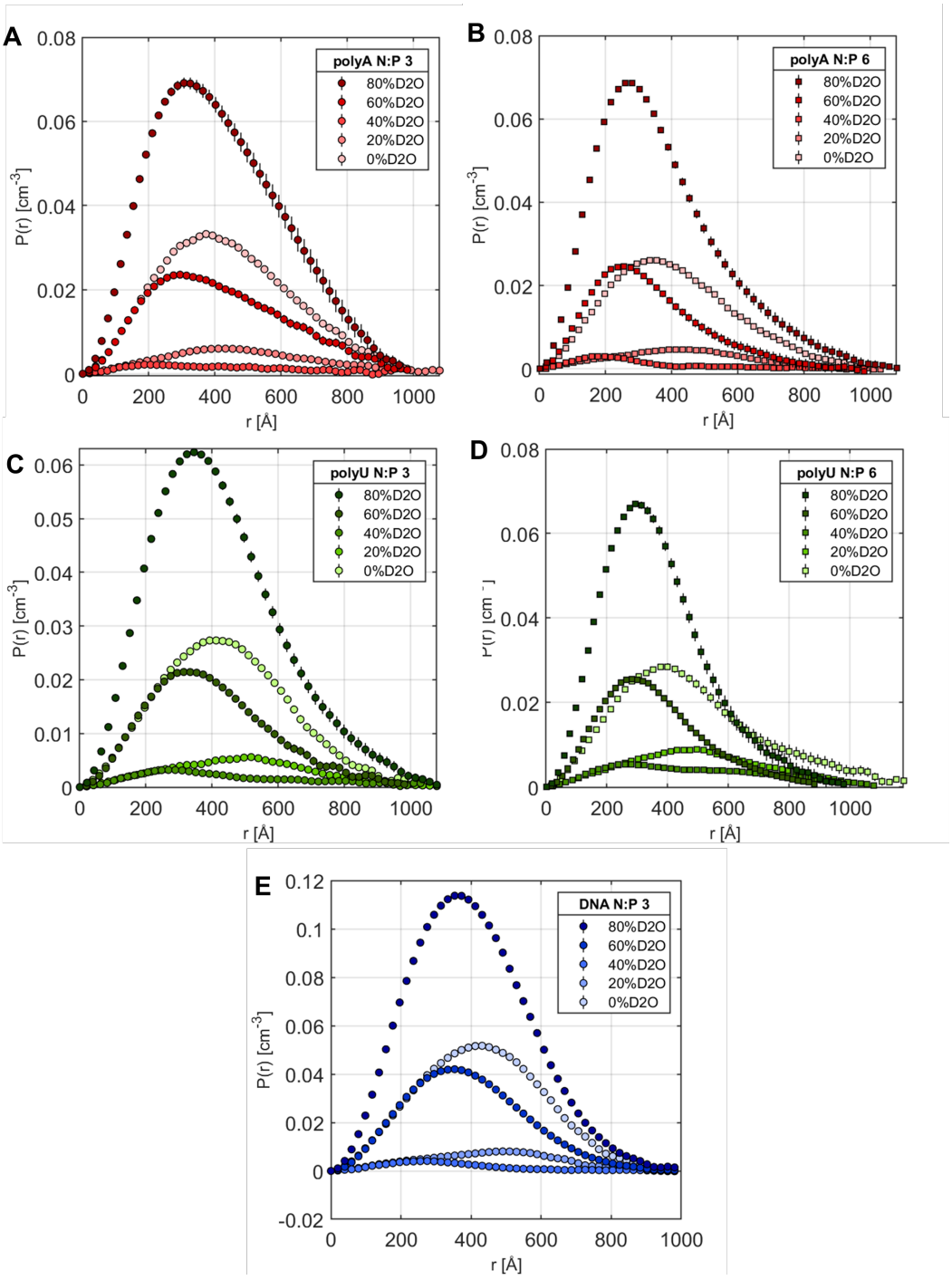

Figure S7: Distance distribution functions, P(r), plotted for LNPs containing polyA N:P 3 (A) and 6 (B), polyU N:P 3 (C) and 6 (D) and DNA N:P 3 (E). All samples were measured in five different solvent contrasts: 0, 20, 40, 60, 80% D_2O (plotted with light to dark colours for increasing D_2O amount).

Table S5: The <Z> hydrodynamic radius R_H measured by DLS immediately after formulation (Day 1) and when the SANS data were measured (Day 4) is presented with the polydispersity index (PDI) in brackets. For DLS, the error is the standard deviation of 6 measurements. For the R_g value determined from the Guinier analysis, the error was determined from the 95% confidence interval on the slope of the linear fit.

Sample	**Contrast (%D_2O)**	**R_H (PDI) /Å**		**R_g from Guinier /Å**	**R_g from P(r)/Å**
		Day 1	**Day 4**		
polyA N:P 3	0	520±10 (0.142±0.004)	520±10 (0.143±0.004)	450±40	340
	20	-	-	550±30	384
	40	-	-	400±300	325
	60	-	-	500±40	329
	80	-	-	420±20	321
polyA N:P 6	0	410±10 (0.118±0.004)	420±10 (0.124±0.004)	300±100	316
	20	-	-	360±70	333
	40	-	-	500±100	259
	60	-	-	300±100	260
	80	-	-	340±30	291
polyU N:P 3	0	390±10 (0.0620±0.005)			339
	20	-	-	-	377
	40	-			354
	60	-			311
	80	-			326
polyU N:P 6	0	350±10 (0.060±0.007)			376
	20	-	-	-	391
	40	-			381
	60	-			278
	80	-			284
DNA N:P 3	0	460±10 (0.050±0.005)	460±10 (0.060±0.007)	390±20	330
	20	-	-	550±30	340
	40	-	-	400±100	274
	60	-	-	320±60	300
	80	-	-	400±10	307

(i) For each sample, the radius and thickness were constrained to be the same and fitted simultaneously for all solvent contrasts (D_2O/H_2O ratios for that sample).

(ii) Shell and core SLDs were fitted simultaneously for each solvent contrast

After initial fitting with the CSS model over the limited range, the combined CSS+BP model was fitted to each dataset over the full q range. All structural parameters from the CSS fit were kept the same and the peak structural parameters for the broad peak model were estimated from the SAXS data for the corresponding sample. The porod exponent was estimated from the data and fixed (2.3), the lorentz exponent was fixed (2), then the scale of the lorentz peak, shell SLD and core SLD were then allowed to fit.

The volume fraction of solvent and dry SLD of the shell and core, respectively, were calculated from the fitted shell and core SLDs for each solvent contrast as follows:

$$SLD_{wet} = (vf_{solvent} SLD_{solvent}) + ((1 - vf_{solvent}) SLD_{dry}) \quad (3)$$

The calculated dry SLDs and solvent volume fractions for the core and shell were the mean of these calculated values with standard deviation given as the error.

Table S6: Table of the core-shell sphere fit parameters for the core-shell sphere plus broad peak model.

Model: CSS+BP	$\mathbf{vf}_{shell}$	$\mathbf{SLD}_{dry-shell}$ $/\mathbf{10^{-6}\text{Å}^{-2}}$	$\mathbf{vf}_{core}$	$\mathbf{SLD}_{dry-core}$ $/\mathbf{10^{-6}\text{Å}^{-2}}$	**Core radius /Å**	**Shell thickness /Å**	**PDI**
polyA N:P 3	0.37±0.09	3.1±0.2	0.33±0.05	1.0±0.1	215±1	45±1	0.23
polyA N:P 6	0.39±0.09	3.8±0.1	0.17±0.03	0.70±0.05	210±1	50±1	0.28
polyU N:P 3	0.32±0.09	3.2±0.2	0.43±0.05	0.9±0.1	295±1	49±1	0.22
polyU N:P 6	0.4±0.1	3.6±0.4	0.29±0.09	0.7±0.2	242±1	49±1	0.22
DNA N:P 3	0.1±0.2	2.9±0.3	0.29±0.05	0.84±0.09	288±1	48±1	0.17

Table S7: Table of the broad peak fit parameters for the core-shell sphere plus broad peak model.

Model: CSS+BP	porod_scale	lorentz_length	peak_pos
polyA N:P 3	$4x10^{-3}$	30±3	0.11±0.01
polyA N:P 6	$1x10^{-3}$	20±3	0.11±0.01
polyU N:P 3	$2x10^{-3}$	20±3	0.11±0.01
polyU N:P 6	$1x10^{-3}$	20±3	0.11±0.01
DNA N:P 3	$1x10^{-5}$	35±1	0.089±0.002

Calculating lipid composition of the shell and core

The lipid composition of the core and shell was determined using the method described by Sebastiani et al.[9] In summary, the molecules in the LNP partition between the shell and core. Considering the molecular volume of each components and the available volume of core and shell, the molecules can be partitioned such that the calculated SLDs match the fitted SLDs. The volume fraction can then be recalculated to a molar fraction using the molecular volume of each component. It should be noted that the composition was calculated assuming that the input lipid molar ratio was conserved and taking into account the encapsulation efficiency measured by RiboGreen assay. It was assumed that all DSPC and PEG lipid were present in the shell and that all NA was in the core.

Effect of temperature

Additional SANS and SAXS measurements were performed to determine the temperature sensitivity of the LNP structure for the different LNP cargos. For the stock solution of polyU N:P 6 (Figure S9D), there was a small decrease in intensity with increasing temperature, possibly a result of increased aggregation and sedimentation with increasing temperature, and decreased definition of the shoulder at $0.015Å^{-1}$ at the highest temperature (65°C), which could be linked to decreasing order in the shell as this is above the chain melting temperature of DSPC.[10]

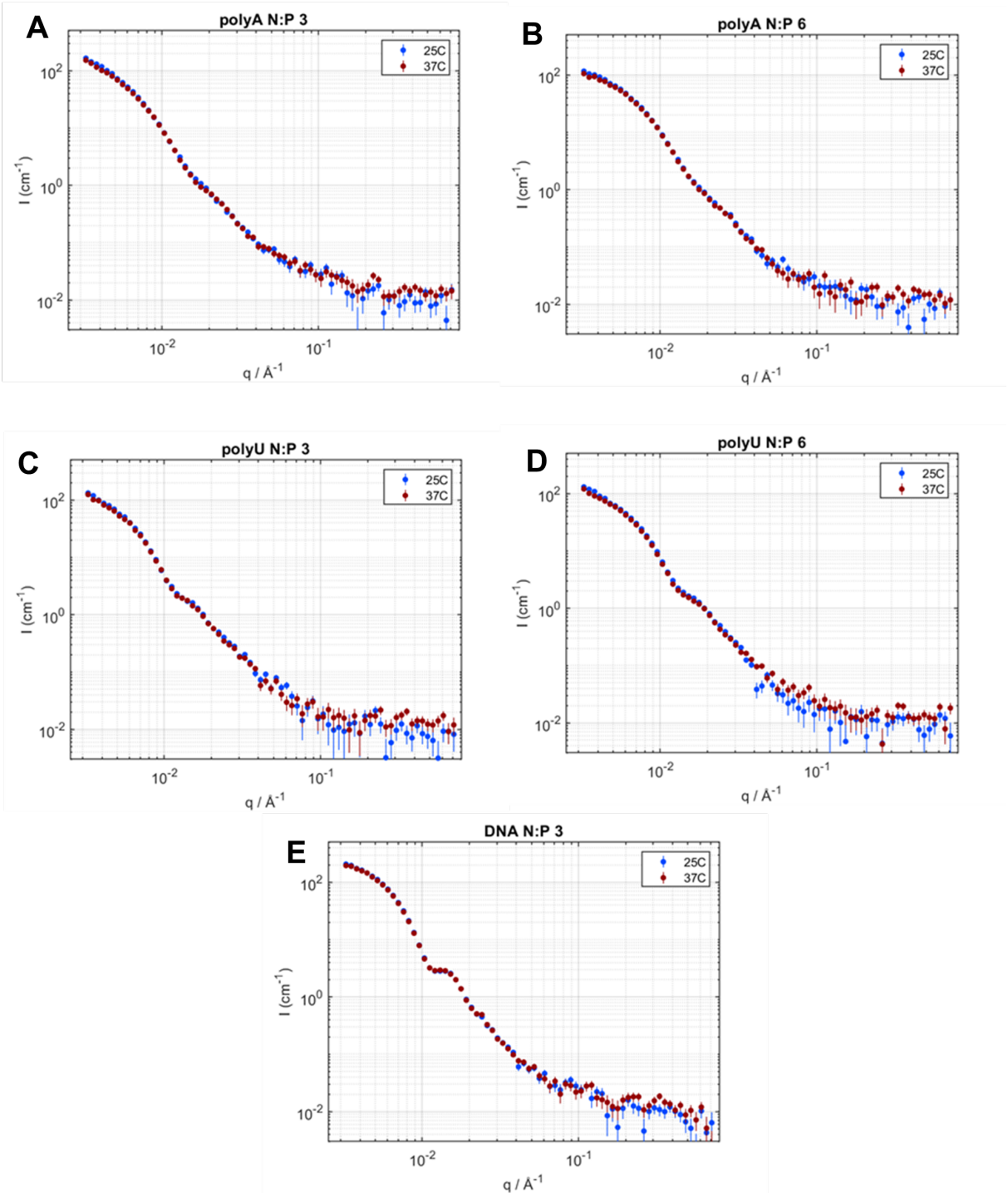

Figure S8: SANS curves for all samples in 0% D_2O contrast at 25 and 37 °C.

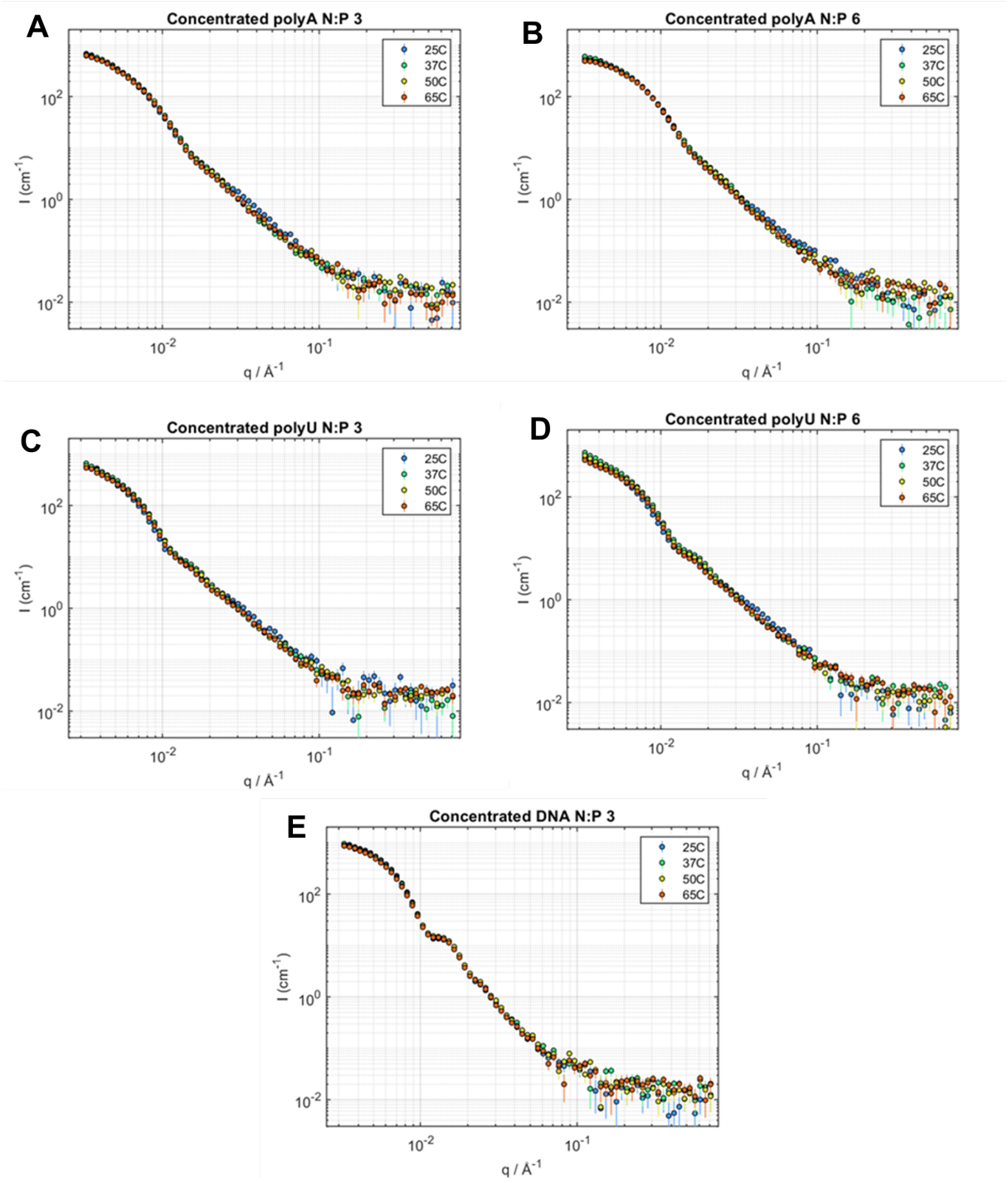

Figure S9: SANS curve for LNP stock solutions in 0% D_2O contrast at 25, 37, 50 and 65 °C.

Static SAXS fitting

Fitting empty LNP data

The empty LNP data kindly provided from a previous work by Yanez Arteta et al.[2] was initially fit with the broad_peak model. The following parameters were fixed: lorentz_exp (2) and scale (1). The background was fitted initially, then fixed. All other parameters were allowed to vary.

Although this provided a good description of the main peak, there appeared to be a second order peak at higher q which was not well described. In order to capture this, a broad_peak model (with parameters defined as above) + a Gaussian peak (all parameters were allowed to vary) was fitted to the data. Although it was possible to manually get a good description of the peak, when the model was allowed to fit, the fit wasn't sensitive to it. When included in the later peak fits of the NA LNPs, the additional peak did not improve the fit and the scale factor went to ≈ 0, therefore the broad_peak fit was used for all sample fitting.

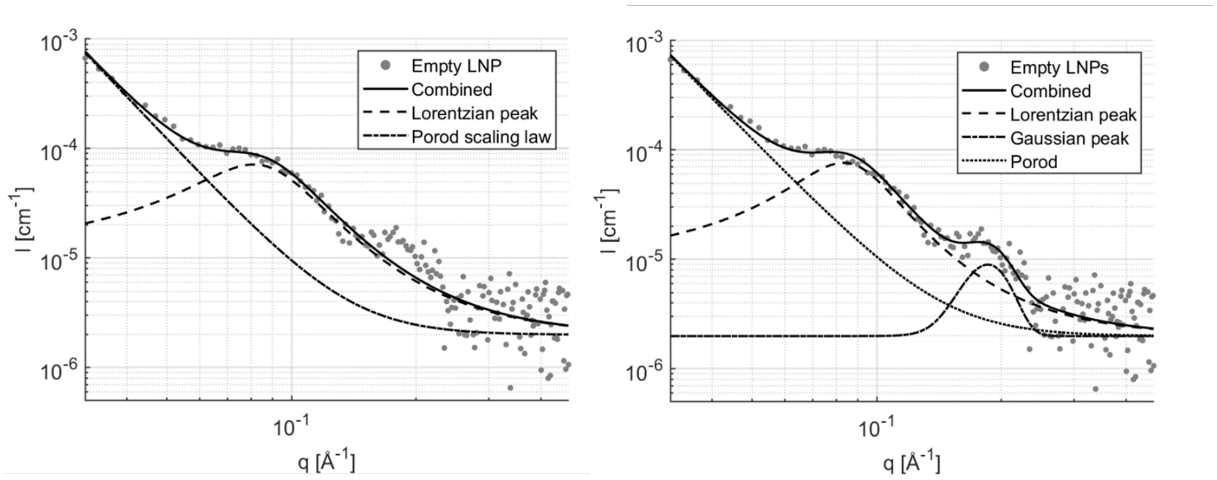

Figure S10: Comparing fit using a broad peak model or a broad peak model plus a Gaussian peak for the SAXS data for empty LNPs.

Table S8: Fit parameters for the empty LNP SAXS data comparing the broad peak model to the broad peak model plus a Gaussian peak.

Empty LNPs	broad_peak	broad_peak+Gaussian
broad_peak		
porod_scale±1x10^{-9}	7.572x10^{-6}	8.607x10^{-6}
porod_exp±0.01	4.00	3.86
lorentz_scale±1x10^{-9}	6.9749x10^{-5}	7.4670x10^{-5}
lorentz_length±0.2 /Å^{-1}	33.4	39.6
peak_pos±0.0001 /A^{-1}	0.08103	0.08307
Gaussian		
scale±1x10^{-8}	-	7.00x10^{-6}
peak_pos±0.001 /Å^{-1}	-	0.186
sigma±0.002 /A^{-1}	-	0.219

Fitting samples: Empty LNP + Gaussian peak

The polyA N:P 3 and 6 and polyU N:P 6 samples were fitted with a combination of the broad_peak model and a Gaussian peak. The broad peak parameters were fixed from the empty LNP fit results (porod_exp, lorentz_length, peak_pos, lorentz_exp) with only the scale parameters allowed to vary (porod_scale, lorentz_scale). All parameters for the Gaussian peak were allowed to vary.

Table S9: Fit parameters for the broad peak plus one Gaussian peak fits to the SAXS data for the polyA samples and polyU N:P 6.

Broad peak + Gaussian	polyA N:P 3	polyA N:P 6	polyU N:P 6
Broad peak			
porod_scale±1x10^{-10}	8.30x10^{-8}	1.007x10^{-7}	6.60x10^{-8}
lorentz_scale±0.0001	0.0476	0.0273	0.0356
Gaussian Peak 1			
scale±0.0001	0.0664	0.0279	0.0149
peak_pos±0.001 /Å^{-1}	0.110	0.110	0.111
sigma±0.001 /A^{-1}	0.012	0.012	0.017

Fitting samples: Empty LNP + 2 Gaussian peaks

For the DNA sample, a single Gaussian peak did not describe the position of the main peak well, due to the contribution from a shoulder on the higher q side of the main peak. For the

polyU N:P 3 sample, there was a clear contribution from a sharp Bragg peak, which could not be described with only 1 Gaussian peak in addition to the broad peak model for the empty LNPs. These samples were therefore fitted with a combined model of the broad_peak model + 2 Gaussian peaks. For comparison, the polyU N:P 6 sample was also originally fitted with a broad peak + 2 Gaussian peak model, but the second peak contribution went to 0, therefore was effectively fitted as a single Gaussian peak.

Table S10: Fit parameters for the broad peak plus two Gaussian peak fits to the SAXS data for the DNA samples and polyU N:P 3.

Broad peak + 2 Gaussians	**polyU N:P 3**	**DNA N:P 3**
Broad peak		
porod_scale±1x10^{-10}	3.92x10^{-8}	5.04x10^{-8}
lorentz_scale±0.0001	0.0285	0.0354
Gaussian Peak 1		
scale±0.0001	0.0327	0.0904
peak_pos±0.001 /Å^{-1}	0.112	0.106
sigma±0.001 /A^{-1}	0.016	0.011
Gaussian Peak 2		
scale±0.0001	0.0673	0.0103
peak_pos±0.001 /Å^{-1}	0.119	0.122
sigma±0.001 /A^{-1}	0.003	0.015

Encapsulation efficiency

Table S11: Encapsulation efficiency of the LNP formulations measured using the Invitrogen Ribogreen assay.

Sample	**Encapsulation efficiency/%**
polyA N:P 3	85
polyA N:P 6	96
polyU N:P 3	80
polyU N:P 6	78
DNA N:P 3	88

References

(1) Cheng, M. H. Y.; Leung, J.; Zhang, Y.; Strong, C.; Basha, G.; Momeni, A.; Chen, Y.; Jan, E.; Abdolahzadeh, A.; Wang, X.; Kulkarni, J. A.; Witzigmann, D.; Cullis, P. R. Induction of Bleb Structures in Lipid Nanoparticle Formulations of mRNA Leads to Improved Transfection Potency. *Advanced Materials* **2023**, *n/a*, 2303370, https://doi.org/10.1002/adma.202303370.

(2) Arteta, M. Y.; Kjellman, T.; Bartesaghi, S.; Wallin, S.; Wu, X.; Kvist, A. J.; Dabkowska, A.; Székely, N.; Radulescu, A.; Bergenholtz, J.; Lindfors, L. Successful reprogramming of cellular protein production through mRNA delivered by functionalized lipid nanoparticles. *Proceedings of the National Academy of Sciences* **2018**, *115*, E3351–E3360.

(3) Greenwood, A. I.; Tristram-Nagle, S.; Nagle, J. F. Partial molecular volumes of lipids and cholesterol. *Chemistry and physics of lipids* **2006**, *143*, 1–10.

(4) Armen, R. S.; Uitto, O. D.; Feller, S. E. Phospholipid component volumes: determination and application to bilayer structure calculations. *Biophysical journal* **1998**, *75*, 734–744.

(5) Wilkinson, D. A.; Nagle, J. F. Dilatometry and calorimetry of saturated phosphatidylethanolamine dispersions. *Biochemistry* **1981**, *20*, 187–192, doi: 10.1021/bi00504a031.

(6) Guinier, André La diffraction des rayons X aux très petits angles : application à l'étude de phénomènes ultramicroscopiques. *Ann. Phys.* **1939**, *11*, 161–237.

(7) Svergun, D. I.; Koch, M. H. J. Small-angle scattering studies of biological macromolecules in solution. *Reports on Progress in Physics* **2003**, *66*, 1735.

(8) Glatter, O.; Kratky, O. *Small Angle X-ray Scattering*; London Academic Press, 1982.

(9) Sebastiani, F. et al. Apolipoprotein E Binding Drives Structural and Compositional Rearrangement of mRNA-Containing Lipid Nanoparticles. *ACS Nano* **2021**, *15*, 6709–6722, doi: 10.1021/acsnano.0c10064.

(10) Silvius, J. R. Thermotropic phase transitions of pure lipids in model membranes and their modifications by membrane proteins. *Lipid-protein interactions* **1982**, *2*, 239–281.